THE POLY(ESTER AMINE)S FUNCTIONAL MAGNETIC CARBON NANOTUBES AS EFFICIENT GENE VECTOR

Q. ZHANG[*], Z. LONG, H.L. FU, G.P. YAN, L. LI
School of Materials Science and Engineering, Wuhan Institute of Technology, Wuhan 430205, People's Republic of China

Magnetic carbon nanotubes have been attracted great interest in biomedicine fields because of their unique structure and magnetic properties. A poly(ester amine)s functional magnetic CNT (CNTs/Fe$_3$O$_4$-HPEI) was prepared and used as gene carrier. The structure was confirmed by FTIR, XRD, TEM, and TGA. The poly(ester amine)s functional magnetic CNTs displayed typical superparamagnetic behavior. Plasmids can be bound by this poly(ester amine)s functional magnetic CNTs to form the nano complexes with positive charge. The gene transfection efficiency is related to the w/w ratio of CNTs/Fe$_3$O$_4$-HPEI and DNA. At the optimal w/w ratio of above 6, the poly(ester amine)s functional magnetic CNTs show a comparable transfection activity to 25k PEI, however the cytotoxicity is much lower. In addition, the gene transfection level can be improved in the magnetic field because of the increased cell internalization rate by magnetic force. These results suggest that the poly(ester amine)s functional magnetic CNTs would be a potential gene vector in targeted gene therapy.

1. Introduction

Gene therapy is a novel revolutionary approach to the treatment of human diseases. It can be used to treat diseases that are serious threats to human health and difficult to cure completely, such as genetic diseases, malignant tumors, cardiovascular diseases, etc [1, 2]. Since DNA is easily degraded by nucleases in the body, carrier transport is required. Gene vectors can be divided into viral and non-viral gene vectors. Viral vectors have high transfection efficiency, and they are the main carriers of gene therapy programs for clinical research [3, 4]. However, due to their immunogenicity, limited in the size of carrying DNA and expensive treatment costs, which restricts their large-scale application. On the other hand, non-viral vectors are gaining more and more attention due to their strong DNA bind ability, lack of immunogenicity, and low cost. However, the transfection activity of non-viral vectors is lower compared with viral vectors, and most of them have certain cytotoxicity, which is difficult to meet the requirements of clinical

---

[*] Corresponding author: booyou@163.com

application [5, 6]. The lack of safe and efficient gene vectors has always been one of the bottlenecks restricting the development of gene therapy.

Magnetic carbon nanotubes (CNTs) are novel one-dimensional materials, which have been extensively applied in many fields because of their excellent physical and chemical properties [7-10]. In the biomedical field, CNTs have been explored as nanocarriers in medicine, because they have a special ability to cross the cell membrane and favorable pharmacokinetics [11]. In addition, thanks to their unique physicochemical architecture, which can bind small interfering RNA (siRNA) and single-strand DNA via non-covalent interactions, CNTs have been used as gene vectors successfully [12]. However, in order to bind double-strand DNA, CNTs are usually be functionalized with cationic polymer to improve the DNA binding ability. The commonly used polycations are polyethyleneimine (PEI) [13, 14], polyamidoamine (PAMAM)[15, 16], chitosan [17] and so on. Among them, PEI is the most popular one because of its high transfection activity. It was reported that high-molecular-weight PEI, such as the Mw of 600k and 25k, modified multiwalled carbon nanotubes have higher gene transfection efficiency than that of PEI alone [13, 18].

Although the high-molecular-weight PEI functionalized CNTs gene vectors displayed high transfection efficiency, their toxicity could not be ignored. It is well known that CNTs can cause toxicity because of highly hydrophobicity. The levels of toxicity are related to their manufacturing method, purity, aspect ratio, functional groups, and so on [19]. Some researchers found that the functionalization of PEI could reduce the cytotoxicity of CNTs. Because this modification could improve the solubility in aqueous media [18]. Nevertheless, high-molecular-weight PEI is also high cytotoxicity, which limits its application as gene vectors. Although the cytotoxicity of low-molecular-weight PEI is relatively low, the transfection activity is poor. They are also not good moiety to modify CNTs for gene delivery. In order to reduce the cytotoxicity of PEI, but do not affect its transfection activity, some degradable PEI derivatives have been synthesized [20, 21]. These PEI derivatives can condense DNA effectively thus display high transfection activity. After transfection, they can be biodegraded to low-molecular-weight PEI to reduce the cytotoxicity. Some disulfide or ester bond containing PEI derivatives exhibit higher transfection efficiency than 25 K PEI, however, the cytotoxicity is rather lower [22, 23].

Lack of targeting specificity is one of the factors limiting the application of non-viral gene vectors. In order to deliver the DNA to specific target cells, some strategies were carried out. The use of magnetic nanoparticles to assist gene delivery is an effective and convenient method [24-26]. In the influence of the magnetic field, more DNA complexes can rapidly aggregate to the target cells, which facilitates endocytic processes, thus increasing the transfection efficiency. Fe_3O_4 is one of the classic magnetic nanoparticles. Due to its excellent magnetism, biocompatibility, and biodegradability, it has been widely used in drug delivery, magnetic resonance imaging (MRI), biochemical separations, and so on [27, 28]. However, the Fe_3O_4 nanoparticles are easy to aggregate because of high surface energy, which is unfavorable for biomedical applications. To improve the stability in suspension, some stabilizers were used to coat on the surface of Fe_3O_4 nanoparticles. The dispersion of Fe_3O_4 nanoparticles in CNTs is effective to prevent them from gathering and maintain superparamagnetism. The magnetic CNTs (MCNTs) have been explored as targeted drug/gene delivery carriers [29, 30].

In the present study, A poly(ester amine)s functional magnetic carbon nanotubes (MCNTs-HPEI) were prepared as gene vectors. The poly(ester amine)s and Fe_3O_4 provide the DNA condense ability and magnetic targeted property, respectively. The structure and composition were investigated using Fourier transform infrared spectroscopy, X-ray diffraction, transmission electron microscopy, X-ray photoelectron spectroscopy, and thermogravimetric analyzer. The cytotoxicity of the MCNTs-HPEI is expected to be lower than the ones modified by 25k PEI. Finally, the magnetically induced cell internalization and gene transfection were investigated.

2. Experimental and methods

2.1. Materials

Carboxyl functionalized multi-wall carbon nanotubes (CNTs-COOH) were obtained from the Chinese Academy of Sciences Chengdu Organic Chemicals Co., LTD. The purity is 98 wt% and contains 1.23 wt% carboxyl groups. The length is 0.5- 2 μm and the outer diameter is 20-30 nm. 1.8k PEI（Mw=1.8 kDa）and 25k BPEI（Mw=25 kDa） were obtained from Sigma-Aldrich. 1-ethyl-3-(3-dimethylaminopropyl) carbodiimide hydrochloride (EDC), N-hydroxysuccinimide (NHS) were purchased from Aladdin Co. (Shanghai, China). Acrylic acid, cyclohexane, 1,6-hexanediol, triethylamine, dimethyl sulfoxide (DMSO), ammonium hydroxide, sodium bicarbonate, ferrous chloride tetrahydrate, ferric chloride hexahydrate, and hydroquinone were purchased from Shanghai Chemical Reagent Company and were used as received. 3-[4,5-dimethylthiazol-2-yl]-2,5-diphenyltetrazoliumbromide (MTT) was purchased from Invitrogen. Dulbecco's Modified Eagle's Medium (DMEM) and penicillin-streptomycin were purchased from Gibco. Fetal bovine serum (FBS) was purchased from Hyclone. Luciferase Assay System was purchased from Promega.

Hela and COS-7 cells were incubated in DMEM containing 10% FBS at 37 °C and humidified air/5% CO_2. The plasmids DNA of pEGFP-C1 and pGL3-Luc were purchased from Genewiz (Suzhou, China).

2.2. Preparation of Magnetic CNTs.

The magnetic CNTs/Fe_3O_4 nanocomposites were fabricated according to our previous study. Briefly, 0.4 g carboxyl CNTs were added in 40 mL deionized water and sonicated at 50 °C for 60 min. Then, 0.184 g $FeCl_3 \cdot 6H_2O$ and 0.068 g $FeCl_2 \cdot 4H_2O$ were added to the solution under nitrogen protection and 10 mL ammonium hydroxide (8 M) was added dropwise. After the reaction at 50 °C for 30 min, the black precipitation was filtered and washed to a pH of 7 with deionized water. Then the product was dried for 24 h in oven at 80 °C.

2.3. Synthesis of 1,6-Hexanediol Diacrylate Linked PEI (HPEI)

1.8g of 1.8k PEI was dissolved in 12 mL DMSO, and then the solution was added to a 50 mL three-necked flask equipped with a condensing device and protected with nitrogen. 0.275 g of 1,6-hexanediol diacrylate was dissolved in 10 mL DMSO, and the 1,6-hexanediol diacrylate solution was added dropwise to the three-necked flask, then the reaction was taken at 45 °C for 48 h. Subsequently, the product was dialyzed against distilled water (MWCO: 3500) for 48 h to remove the unreacted 1.8 kDa PEI. Finally, HPEI was obtained by free-drying for 48 h.

2.4. Synthesis of CNTs/Fe_3O_4-HPEI

0.2g magnetic CNTs/Fe_3O_4 nanocomposites were suspended in 20 mL distilled water and ultrasonically dispersed for 30 min at 50 °C. Then 0.105 g EDC and 0.082 g NHS were added to activate the carboxyl groups. Subsequently, the HPEI solution (0.2 g HPEI dissolved in 2 mL distilled water) was added and stirred for 24 h at room temperature. After the reaction, the product was centrifuged at 20,000 × g for 15 min, then re-dispersed in distilled water and dialyzed

(MWCO:12000) for 48 h to remove the unreacted HPEI and activating agent. Lastly, the solution was lyophilized for 48 h to obtain CNTs/Fe$_3$O$_4$-HPEI in a black powdered form.

2.5. Characterization of CNTs/Fe$_3$O$_4$-HPEI

Fourier transform infrared (FT-IR) spectra of CNTs/Fe$_3$O$_4$-HPEI was recorded on Nicolet Impact-420 Fourier transform infrared spectrometer in the range of 400 - 4000 cm^{-1}. X-ray diffraction patterns were obtained by Bruker D8 Advance X-ray powder diffractometer using $K\alpha$ ($\lambda = 1.5404$), the scanning range is 10 to 90 degrees. The morphology of CNTs/Fe$_3$O$_4$-HPEI was conducted by JEM-2100F field emission electron microscopy (TEM, JEOL, Japan). Thermogravimetric analyzer (TGA) measurement was performed by a TGA STA-409PC thermogravimetric analyzer under N$_2$ in the temperature range 30-800 ˚C with an increasing rate of 5 ˚C min^{-1}. The magnetic properties were measured using a vibrating specimen magnetometer (Squid-VSM) to the field strength of 20 KOe at room temperature.

2.6. Preparation of Vector/DNA Complexes

To prepare CNTs/Fe$_3$O$_4$-HPEI and DNA complexes, 50 μL DNA solution (containing 1 μg pEGFP-C1 or pGL3-Luc) and 50 μL CNTs/Fe$_3$O$_4$-HPEI solution were mixed at various w/w ratios of CNTs/Fe$_3$O$_4$-HPEI to DNA, then vortexed and incubated for 20 min.

The PEI/DNA complexes at the N/P ratio of 10 were prepared as following, 50 μL DNA solution (containing 1 μg pEGFP-C1 or pGL3-Luc) and 50 μL PEI solution (containing 1.33 μg PEI) were mixed. Then the mixture was vortexed and incubated for 20 min.

2.7. Size and Zeta Potential Measurements

The mean size and surface charge were determined by a Zetasizer Nano-ZS (Malvern, ZEN3600, UK). CNTs/Fe$_3$O$_4$-HPEI/DNA complexes solution (containing 5 μg pGL3-Luc) was diluted to1 mL, then to take the measurement. The mean ± standard deviation (SD) was given according to three independent measurements.

2.8. In Vitro Cytotoxicity

The cytotoxicity of CNTs/Fe$_3$O$_4$-HPEI and 25k PEI were examined by the MTT assay. COS-7 cells were seeded in 96-well plates at a density of 6×10^3 cells per well and cultured for 24 h. Then the medium was replaced with a fresh medium containing a certain concentration of CNTs/Fe$_3$O$_4$-HPEI or 25k PEI. The concentration ranges from 0 to 100 μg/mL. After cultured for 48 hours, the medium was removed. 200 μL fresh medium and 20 μL of MTT (5 mg/mL) were added to each well, then continue incubated for 4 h. The supernatant was carefully discarded, then150 μL of DMSO was added to each well, and gently shaken for 5 min to dissolve the blue-purple formamidine crystal obtained by reducing MTT from succinate dehydrogenase in living cell mitochondria. The OD value of each well was recorded at 570 nm using a microplate reader (Bio-Rad 550).

Cell viability is calculated by the following formula:

Cell viability = OD$_{sample}$ / OD$_{control}$ × 100%

Where the OD$_{sample}$ was obtained by the well with CNTs/Fe$_3$O$_4$-HPEI or 25 kDa PEI, and OD$_{control}$ was obtained by the well without CNTs/Fe$_3$O$_4$-HPEI or 25 kDa PEI.

2.9. In vitro transfection

Luciferase assay

COS-7 cells or Hela cells were directly seeded into 24-well plates at a density of 5×10^4 cells per well. After cultured for 24 h, the medium was removed, and 900 μL of serum-free DMEM was added. 100 μL CNTs/Fe$_3$O$_4$-HPEI/DNA complexes prepared according to the preceding method was added. Then a magnet (0.2 T, M+) was placed under the plate. The transfection was occurred without the magnet (M-) as a contrast. After incubation for a certain time, the medium was replaced with fresh medium. And the cells were further incubated for 44 h. Then the medium was removed, and the cells were gently washed 3 times with phosphate buffer (PBS, pH 7.4). The cells were completely lysed by 200 μL of lysate (Promega) per well. After centrifugation, the cell lysis supernatant (20 μL) was thoroughly mixed with a luciferase substrate (Promega, 100 μL), and the activity of luciferase was measured by a luminometer (Lumat LB9507, Berthold). The protein concentration in the cell lysate were measured using a BCA protein assay reagent kit (Pierce), the OD value of the solution at 570 nm was measured with a microplate reader (Bio-rad 550). The transfection efficiency was expressed by luciferase activity in RLU per mg protein.

Green fluorescent protein assay

Another plasmid of pEGFP-C1 was used to evaluate the transfection in COS-7 cells. The transfection process is the same as luciferase assay. The weight ratio of CNTs/Fe$_3$O$_4$-HPEI/DNA complexes is 8. After transfection, the cells expressing green fluorescent protein were recorded by an Olympus IX70 fluorescence inverted-phase contrast microscope equipped with a CCD (Roper CoolSnap Color). The micrographs were obtained at the magnification of 200 ×.

2.10. Cellular uptake study

Firstly, YOYO-1 was used to label pGL-3. Then CNTs/Fe$_3$O$_4$-HPEI/DNA complexes were prepared at w/w ratio of 8. COS-7 cells were seed in a culture dish at a density of 3.0×10^5 with 2 mL medium. After incubated for 24 h, the medium was removed and serum-free DMEM with the CNTs/Fe$_3$O$_4$-HPEI/DNA complexes solution was added. Then the cells were further incubated for 4 h at 37°C in the presence or absence of a magnet. Subsequently, the cells were washed several times with PBS, and the nuclei were stained with Hoechst 33258 for 15 min at 37°C. Then the cells were also washed several times with PBS. At last, the cells were observed by confocal laser scanning microscopy (CLSM Nikon Ni-E C2+) at the magnification of 400 ×.

2.11. Statistical Analysis

The statistical difference between two sets of data were performed by Student's t-test. Results were considered significant difference if $P < 0.05$ (*).

3. Results and discussion

In order to further study the magnetic carbon nanotube gene vector, we prepared a magnetic carbon nanotube functionalized with poly(ester amine)s. First, a polyethyleneimine derivative (HPEI) containing an ester bond was synthesized by using 1,6-hexanediol diacrylate as a crosslinking agent. Then the HPEI was grafted onto the surface of the magnetic carbon nanotubes to obtain an poly(ester amine)s functionalized magnetic carbon nanotubes (MCNTs-HPEI). The synthetic route is shown in Scheme 1.
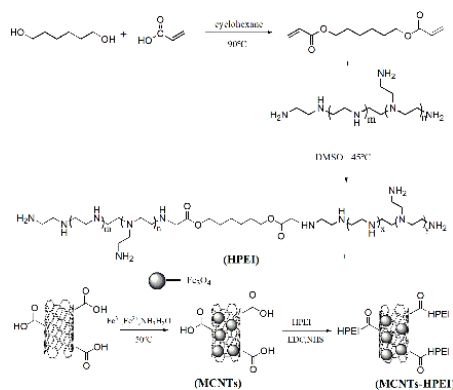
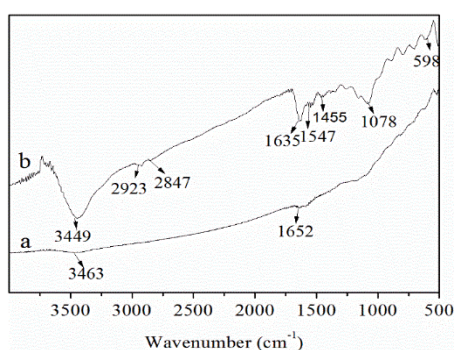*Scheme 1. Schematic illustration of the synthesis of MCNTs-HPEI.*

Fig. 1. FT-IR spectra of carboxyl CNTs (a) and MCNTs-HPEI (b).

3.1. Fourier-Transform Infrared (FT-IR) spectroscopy

The results of FTIR spectroscopy are shown in Fig. 1. In curve a, the -OH and C=O stretching of carboxyl carbon nanotubes were seen at the peak of 3463 cm^{-1} and 1652 cm^{-1}. In curve b, the broad and strong peak at 3449 cm^{-1} is attributed to N-H stretching in CNTs/Fe$_3$O$_4$-HPEI. The peaks at 1635 cm^{-1}, 1547 cm^{-1}, and 1455 cm^{-1} are the characteristic peaks of the amide bond, which confirms the reaction of carboxyl CNTs/Fe$_3$O$_4$ nanoparticles and HPEI [15]. The peak around 600 cm^{-1} is attributed to Fe-O stretching vibrations and it is the characteristic peak of iron oxides.

3.2. X-ray diffraction studies

Fig. 2. shows the X-ray diffraction pattern of CNTs-COOH and MCNTs-HPEI particles. According to the X-ray diffraction data cards (JCPDS No.86-1354), the standard Fe$_3$O$_4$ crystal with spinel structure has six characteristic crystal faces of (220), (311), (400), (422), (511), and (440), which are appeared at 2θ=30.0°, 35.6°, 42.6°, 53.6°, 57.3°, 62.9°. All the peaks are found in the pattern of CNTs/Fe$_3$O$_4$-HPEI particles. Therefore, the iron oxide in the particles is Fe$_3$O$_4$ with spinel structure. The remaining two crystal faces of (002) and (400) belong to carbon nanotubes.
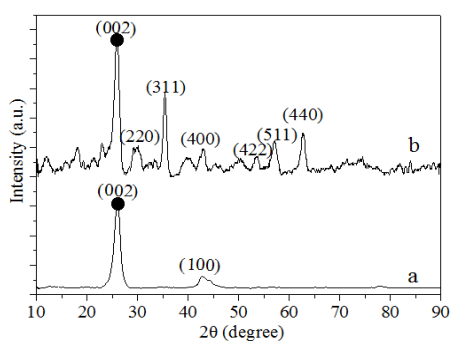
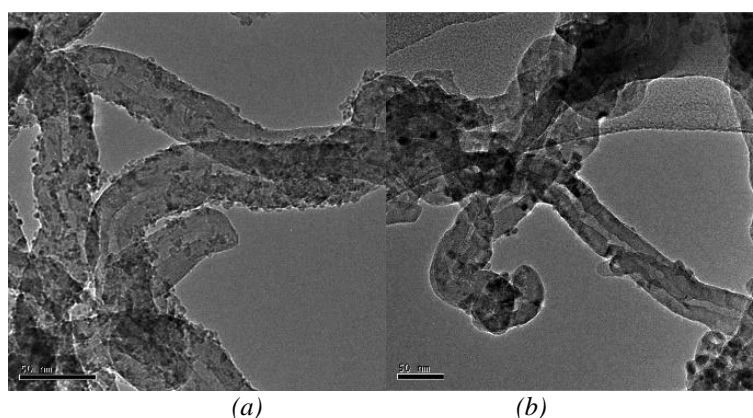Fig. 2. X-ray diffractograms of carboxyl CNTs (a) and MCNTs-HPEI (b).

(a)   *(b)*

Fig. 3. TEM images of MCNTs (a) and MCNTs-HPEI (b).

3.3. Transmission Electron Microscopy

The morphology of CNTs/Fe_3O_4-HPEI magnetic nanoparticles was explored by TEM. As shown in Fig. 3, roughly spherical particles were observed on the surface and inner of the carbon nanotubes and the distribution was uniform. The particles size is ranging from 5 nm to 10 nm. According to the results of XRD analysis, the particles are Fe_3O_4. It has been reported that Fe_3O_4 nanoparticles prepared by coprecipitation are easy to aggregate due to the high surface energy and magnetic pole. However, we can observe clearly that there is no aggregate of nanoscale Fe_3O_4 particles. The Fe_3O_4 particles are attached uniformly on carbon nanotubes. This is because of the interaction of Fe_3O_4 and carbon nanotubes, which prevented the aggregation [12]. As we know, only the size of Fe_3O_4 particles is less than 25 nm, it displays superparamagnetism. Therefore, the nanoscale size is necessary to obtain the superparamagnetism of Fe_3O_4 particles.

3.4. Thermogravimetric analysis (TGA)

Due to the excellent thermal stability of carbon nanotubes and Fe_3O_4, thermogravimetric analysis (TGA) was used to estimate the content of organic components of MCNTs-HPEI. As shown in Fig. 4, all the groups showed slightly weight loss at the stage of the temperature below 200 ℃, this is the result of the evaporation of trace moisture. The significant weight loss was observed in the sample of MCNTs-HPEI nanoparticles at the temperature of 200℃ - 400℃. This is ascribed to the decomposition of HPEI. The content of HPEI in nanoparticles is estimated by TGA is about 37%.
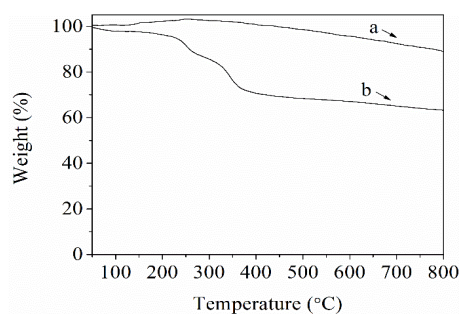
Fig. 4. TGA curve of MCNTs (a) and MCNTs/HPEI (b)

3.5. The magnetic properties

The magnetic properties of CNTs/Fe$_3$O$_4$ and MCNTs-HPEI nanoparticles were tested by Vibrating sample magnetometer. As shown in Fig.5, the hysteresis loops of both nanoparticles display that their coercivity and remanence are close to zero. This is the characteristic of superparamagnetism. The saturation magnetizations of CNTs/Fe$_3$O$_4$ nanoparticles is 12.3 emu/g, which is lower than that of bulk Fe$_3$O$_4$ (about 64 emu/g). The decreased saturation magnetization is due to the small particle size of Fe$_3$O$_4$ and the low content of Fe$_3$O$_4$ in the nanoparticles. The saturation magnetization is further decreased to 6.8 emu/g, when CNTs/Fe$_3$O$_4$ nanoparticles were functionalized with HPEI. Although the saturation magnetization is decreased, they still have good magnetic responsiveness. As shown in Fig. 5b MCNTs-HPEI nanoparticles were aggregated to the magnet within 30 min.
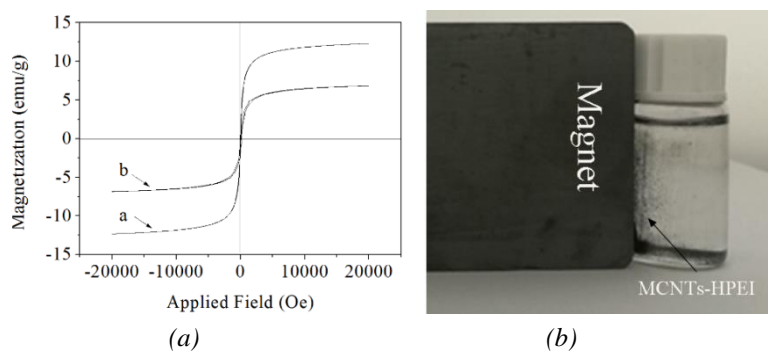

(a)   *(b)*

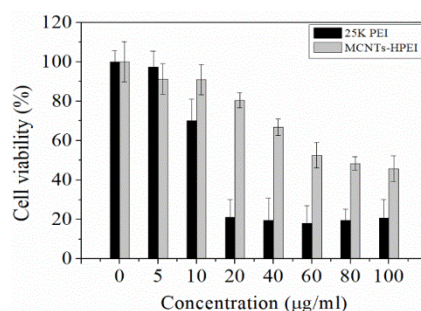*Fig. 5. Magnetization curve of MCNTs (a) and MCNTs/HPEI (b).*

Fig. 6. Cytotoxicity induced by MCNTs/HPEI and PEI (25 kDa) in COS-7 cells.

Data are shown as mean ± SD (n=5).

3.6. Cytotoxicity of MCNTs-HPEI nanoparticles

The cytotoxicity of MCNTs-HPEI and 25 kDa PEI was evaluated on COS-7 cells by MTT assay. The results are shown in Fig. 6. the cell viability of MCNTs-HPEI was over 80 % when the concentration was 20 mg/mL, but the cell viability of 25 kDa PEI was decreased to about 20% at the same concentration. Therefore, the cytotoxicity of MCNTs-HPEI is significantly lower than that of PEI 25 kDa. It has to be noted that the cell viability decreases with the increasing concentration of MCNTs-HPEI, which indicates that MCNTs-HPEI nanoparticles have a certain extent cytotoxicity at high concentrations (>40 ug/mL). This result is similar to that of PEI grafted carbon nanotubes [12,17]. The cytotoxicity is a major obstacle for carbon nanotubes in biological applications. Pristine carbon nanotubes are not suitable to use as gene vector, because they are easy to agglomerate, difficult to disperse in biological medium and not efficiently bind with plasmid DNA. Therefore, some high molecular weight PEI, such as PEI 25k Da and PEI 600 kDa, were used to functionalized carbon nanotubes to improve the DNA binding ability. However, although the high molecular weight PEI have a high positive charge density, which is favorable for binding DNA, they also have ignorable cytotoxicity. They are not the optimal functional molecules. It has been reported that degradable PEI derivatives exhibited lower cytotoxicity at the comparable molecular weight [22,30]. Therefore, the ester bond contained PEI was used to modified magnetic CNTs to obtain decreased cytotoxicity. Our results demonstrate that MCNTs-HPEI has significant lower cytotoxicity than PEI 25 kDa.
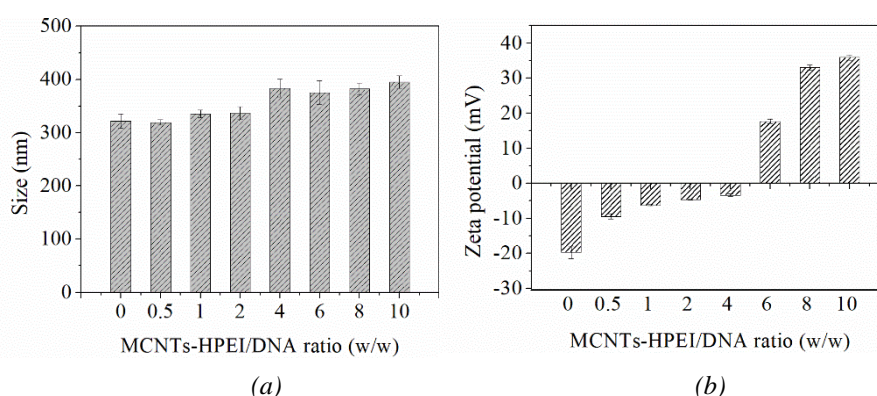

(a)   *(b)*

Fig. 7. The particle sizes (a) and zeta potential (b) of MCNTs-HPEI/DNA particles with different mass ratios of MCNTs-HPEI/DNA. The size of MCNTs-HPEI nanoparticles was measured as control (CON). Data are shown as mean ± SD (n=3).
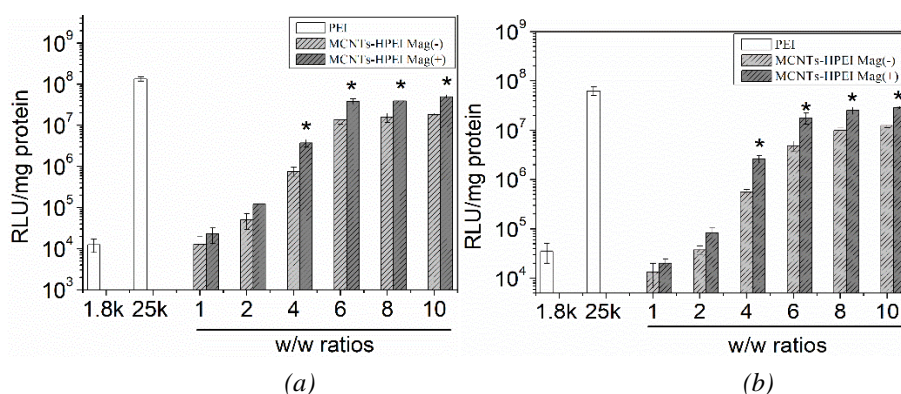
Fig. 8. Fig. 8. The transfection efficiency of MCNTs-HPEI/DNA complexes in COS-7 cells (A) and Hela cells (B). Data are shown as mean ± SD (n=3). (*P < 0.05 as compared with the data at the same w/w ratios without external magnetic field).

3.7. The size and zeta potential of MCNTs-HPEI/DNA complexes

The particle size and surface charge are of importance for cell uptake. A positive surface charge and suitable size of DNA complexes are favorable for negatively charged cell membranes, thus improve cell endocytosis [20]. The size and surface charge of the MCNTs-HPEI/DNA complexes were measured by a Zetasizer Nano-ZS (Malvern, ZEN3600, UK). The results were shown in Fig. 7. The sizes of the complexes are around 400 nm, which are not significantly affected by the weight ratio of MCNTs-HPEI and DNA. This is because that the plasmids are ring-shaped biological macromolecule, the volume is much smaller than MCNTs-HPEI particles. When the complexes were formed between them, the plasmids were attached to the surface of particles and formed a thin film. The size of complexes was determined mainly by the volume of $CNTs/Fe_3O_4$-HPEI particles. Fig. 7b shows the relationship between the zeta potential and the weight ratio of MCNTs-HPEI/DNA. The zeta potentials of complexes increased with the increase of weight ratio (w/w). When the w/w ratio is above 4, the zeta potentials values of $CNTs/Fe_3O_4$-HPEI/DNA complexes changed from negative to positive, indicating all the plasmid DNA were bound with magnetic nanoparticles. The zeta potential of the MCNTs-HPEI/DNA was +27 mV, at the weight ratio of 6.
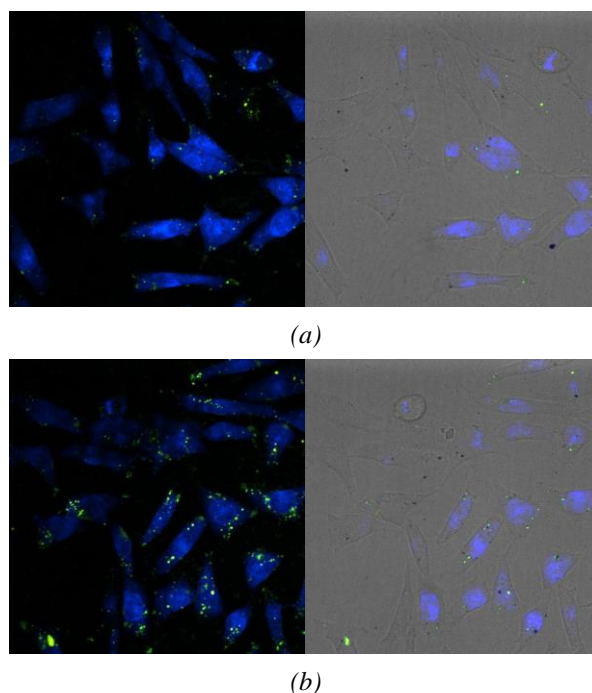
(a)

(b)

Fig. 9. Confocal images of COS-7 cells after incubation with MCNTs-HPEI/DNA nanoparticles (a) and with an external magnetic field (b). The weight ratio of MCNTs-HPEI to DNA is 6.

3.8. Transfection efficiency

Two plasmids of pGL-3 and pEGFP-C1 were used to evaluate the transfection activity of functionalized magnetic CNTs in COS-7 cells and Hela cells. The transfection efficiencies of DNA complex of 1.8K PEI and 25k PEI at the optimal N/P ratio (N/P=10) were used as controls. As shown in Fig. 8, the transfection efficiency of the MCNTs-HPEI/DNA complex gradually increased as the weight ratio increased from 1 to 6. When the w/w ratio is greater than 6, the transfection efficiency did not increase significantly. It was reported that the transfection activity of the DNA complex is related to the surface charge [4,20]. The DNA complex with a high positive charge are more easily to be taken up by cells, due to the interaction with negatively charged cell membrane. Therefore, the increasing transfection activity of MCNTs-HPEI may be attributed to the increased surface charge. However, if the positive charge is too high, the cytotoxicity will increase, which is not conducive to transfection.

Another important finding is when a magnet (0.2T) was added to the bottom of the cell culture plate during the transfection, the transfection efficiency was further increased. For example, at the w/w ratio of 6, the gene expressed in the presence of a magnetic field (RLU/mg protein) was 2.3 times higher than that of the absence of a magnetic field (RLU/mg protein). Under optimal conditions, transfection efficiency is equivalent to 25k PEI. The improved transfection activity of magnetic gene vectors under the extern magnetic field may be the reason that the magnetic gene vector can deposit quickly on the surface of the cells by the induction of a magnetic field. The increased concentration of the magnetic DNA complex at the surface of the cell is a favor to the uptake by cells, thus improves the gene transfection efficiency. The similar phenomena were found in the transfection of Hela cells (Fig. 8b).
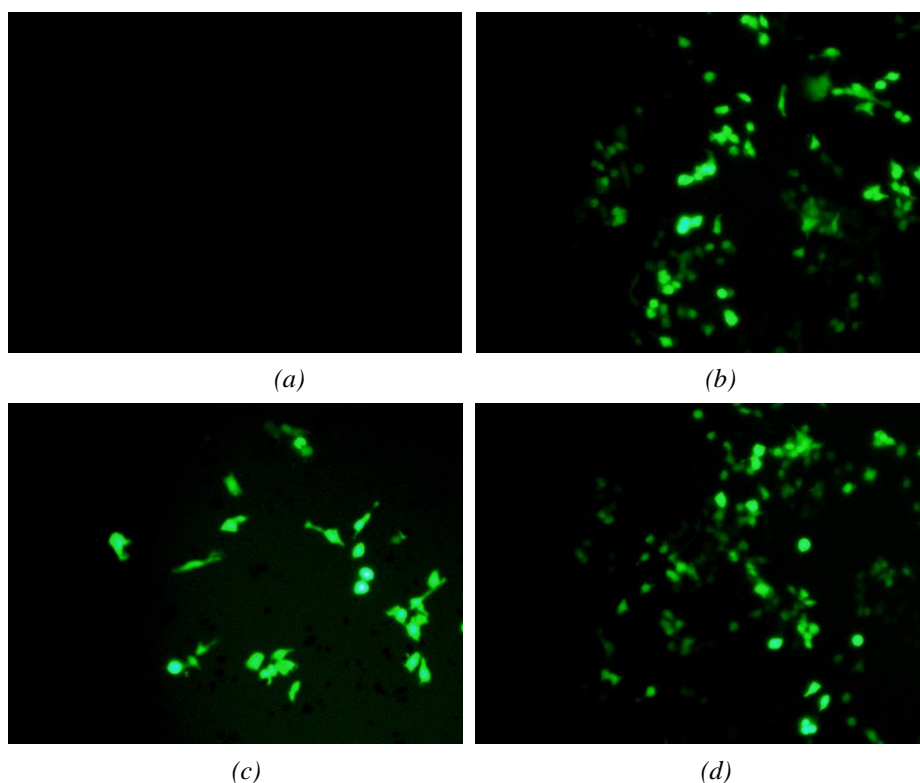
Fig. 10. Enhanced green fluorescent protein expression in COS-7 cells transfected with 1.8 kDa PEI/DNA (a) and 25 kDa PEI/DNA (b) at N/P of 10, as well as CNTs/Fe$_3$O$_4$-HPEI/DNA complexes at weight ratio of 6 without an external magnetic field (c) and with an external magnetic field (d).

In order to confirm this mechanism, the cellular uptake of MCNTs-HPEI/DNA complexes was investigated by laser confocal microscopy. The plasmids were stained by YOYO-1 (green) and the nuclei were stained by Hoechst 33258 (blue). The micrographs were shown in Fig 9. There are more DNA complexes were observed in the cytoplasm in the presence of a magnetic field. It was reported that the internalization of functional-CNTs is probably based on the combination uptake mechanisms of energy independent pathways such as cell penetration, and energy dependent pathways, such as endocytosis or phagocytosis [31] The interaction between magnetic CNTs/DNA complexes and cells can be improved by an external magnetic field. This is helpful for DNA complexes to cross the cell membranes in both uptake mechanisms. Therefore, the cellular uptake rate of the MCNTs-HPEI/DNA complex can be increased by the applied magnetic field, which results in the improvement of transfection efficiency.

Another plasmid pEGFP-C1 was used to further assess the transfection activities of MCNTs-HPEI in COS-7 cells. The transfection results were shown in Fig.10. More green fluorescent dots were observed for the COS-7 cells transfected in the presence of a magnetic field than without magnetic field. It also demonstrates that an external magnetic field can increase the transfection activity of magnetic gene vectors.

3. Conclusions

In this study, the poly(ester amine)s functional magnetic CNTs were prepared. The structure was confirmed by FTIR, XRD, TEM, and TGA. The Fe_3O_4 nanoparticles were distributed uniformly inside or on the surface of the CNTs and the MCNTs-HPEI displayed superparamagnetism. The functionalization of poly(ester amine)s reduced the cytotoxicity of CNTs as well as improved their dispersion in water.

Plasmids can be bound by this poly(ester amine)s functional magnetic CNTs to form the nano complexes with positive charge. The poly(ester amine)s functional magnetic CNTs show a comparable transfection activity to 25k PEI and the cytotoxicity is much lower. In addition, the gene transfection level can be improved in the application of a magnetic field because of the increased cell internalization rate by magnetic force. Therefore, the poly(ester amine)s functional magnetic CNTs would be a potential targeted gene vector.

References

[1] R.C. Mulligan, Science **260**(5110), 926 (1993).

[2] C. E. Dunbar, K. A. High, J. K. Joung, D. B. Kohn, K. Ozawa, M. Sadelain, Science **359**(6372), 175 (2018).

[3] S. L. Ginn, A. K. Amaya, I. E. Alexander, M. Edelstein, M. R. Abedi, Journal of Gene Medicine **20**(5), 16 (2018).

[4] C. E. Thomas, A. Ehrhardt, M. A. Kay, Nature reviews. Genetics **4**(5), 346 (2003).

[5] H. Yin, R. L. Kanasty, A. A. Eltoukhy, A. J. Vegas, J. R. Dorkin, D. G. Anderson, Nature Reviews Genetics **15**(8), 541 (2014).

[6] C. L. Hardee, L. M. Arevalo-Soliz, B. D. Hornstein, L. Zechiedrich, Genes **8**(2), 22 (2017).

[7] R. H. Baughman, A. A. Zakhidov, W. A. de Heer, Science **297**(5582), 787 (2002).

[8] H. Li, F. Pan, Y. Wu, Y. Zhang, X. Xie, Materials Science-Medziagotyra **22**(2), 188 (2016).

[9] M. F. L. De Volder, S. H. Tawfick, R. H. Baughman, A. J. Hart, Science **339**(6119), 535 (2013).

[10] X. Wu, K. Zhang, Y. Zhang, H. Ji, X. Qu, Digest Journal of Nanomaterials and Biostructures **13**(2), 399 (2018).

[11] R. Alshehri, A. M. Ilyas, A. Hasan, A. Arnaout, F. Ahmed, A. Memic, Journal of Medicinal Chemistry **59**(18), 8149 (2016).

[12] K. Bates, K. Kostarelos, Advanced Drug Delivery Reviews **65**(15), 2023 (2013).

[13] Y. Liu, D.-C. Wu, W.-D. Zhang, X. Jiang, C.-B. He, T.S. Chung, S.H. Goh, K.W. Leong, Angewandte Chemie **44**(30), 4782 (2005).

[14] A. H. Nia, A. Amini, S. Taghavi, H. Eshghi, K. Abnous, M. Ramezani, International Journal

of Pharmaceutics **502**(1-2), 125 (2016).

[15] M. Liu, B. Chen, Y. Xue, J. Huang, L. Zhang, S. Huang, Q. Li, Z. Zhang, Bioconjugate Chemistry **22**(11), 2237 (2011).

[16] B. Pan, D. Cui, P. Xu, C. Ozkan, G. Feng, M. Ozkan, T. Huang, B. Chu, Q. Li, R. He, G. Hu, Nanotechnology **20**(12), (2009).

[17] X. Liu, Y. Zhang, D. Ma, H. Tang, L. Tan, Q. Xie, S. Yao, Colloids and Surfaces B-Biointerfaces **111**, 224 (2013).

[18] B. Z. Yu, J. F. Ma, W. X. J. N. P. G. Li, Nature Precedings **1**(1), 2753 (2009).

[19] S. M. Moghimi, P. Symonds, J. C. Murray, A. C. Hunter, G. Debska, A. Szewczyk, Molecular therapy : the journal of the American Society of Gene Therapy **11**(6), 990 (2005).

[20] R. Kircheis, L. Wightman, E. Wagner, Advanced Drug Delivery Reviews **53**(3), 341 (2001).

[21] S. Taranejoo, J. Liu, P. Verma, K. Hourigan, Journal of Applied Polymer Science **132**(25), (2015).

[22] Y.-X. Sun, X. Zeng, Q.-F. Meng, X.-Z. Zhang, S.-X. Cheng, R.-X. Zhuo, Biomaterials **29**(32), 4356 (2008).

[23] Q. Peng, Z. Zhong, R. Zhuo, Bioconjugate Chemistry **19**(2), 499 (2008).

[24] I. Belyanina, O. Kolovskaya, S. Zamay, A. Gargaun, T. Zamay, A. Kichkailo, Molecules **22**(6), (2017).

[25] K. Ulbrich, K. Hola, V. Subr, A. Bakandritsos, J. Tucek, R. Zboril, Chemical Reviews **116**(9), 5338 (2016).

[26] J. Dobson, Gene therapy **13**(4), 283 (2006).

[27] L. Shen, B. Li, Y. Qiao, Materials **11**(2), 324 (2018).

[28] S. Laurent, D. Forge, M. Port, A. Roch, C. Robic, L. V. Elst, R. N. Muller, Chemical Reviews **108**(6), 2064 (2008).

[29] H. Unterweger, R. Tietze, C. Janko, J. Zaloga, S. Lyer, S. Duerr, N. Taccardi, O.-M. Goudouri, A. Hoppe, D. Eberbeck, D. W. Schubert, A. R. Boccaccini, C. Alexiou, International Journal of Nanomedicine **9**, 3659 (2014).

[30] L. Wang, J. Shi, Y. Hao, P. Zhang, Y. Zhao, D. Meng, D. Li, J. Chang, Z. Zhang, Journal of Biomedical Nanotechnology **11**(9), 1653 (2015).

[31] C. Caoduro, E. Hervouet, C. Girard-Thernier, T. Gharbi, H. Boulahdour, R. Delage-Mourroux, M. Pudlo, Acta Biomaterialia **49**(1), 36 (2017).